

Residual modulation of galactic cosmic rays in the heliosphere

Victor Yanke , Anatoly Belov , Raisa Gushchina , Pavel Kobelev , Lyudmila Trefilova 

Correspondence

IZMIRAN – Pushkov Institute of Terrestrial Magnetism, Ionosphere and Radiowave Propagation, Moscow, Russia, yanke@izmiran.ru

Keywords

long-term variations; heliosphere; PAMELA; AMS-02; Voyager-1; ground-based detectors; residual modulation

Abstract

Residual modulation of galactic cosmic rays in the heliosphere and its energy dependence are studied with data from three types of ground-based detectors, using data from PAMELA, AMS-02, and Voyager 1/2. It is shown that the residual modulation is approximately the same in magnitude as the observed variations due to the solar activity cycle, which allows us to make some conclusions about the modulation processes in the heliosphere.

1. Introduction

The concept of residual modulation, introduced at the beginning of the space age (Nagashima et al. 1980), arose when solving the problem of the size of the heliosphere, which has now been determined experimentally. The issue of residual modulation today is more related to the efficiency of the heliosphere as a whole and the contribution of its individual regions. Assuming that at the minimum of solar activity the heliosphere is completely filled with unmodulated galactic cosmic rays (CR), one can expect an insignificant residual modulation, but it is important to know the value of such residual modulation for particles of different energies.

Recent studies have shown that galactic cosmic rays intensity nowadays is significantly lower than in previous centuries (McCracken et al. 2004). The studies carried out in this work show that the sunspots number in the solar activity minima of the last 6 cycles correspond to a modulation potential of about 500 MV, while the potential during the Maunder minimum is < 100 MV. In the complete absence of modulation at the modulation potential $\Phi = 0$ MV, the local interstellar spectrum (LIS) of GCRs would be observed in the Earth's orbit, which would lead to the maximum count rate of detectors on Earth.

A powerful incentive for a detailed study of the modulation of galactic cosmic rays in the heliosphere was the exit of Voyager-1/2 (Stone et al. 2019) beyond the heliosphere, as well as accurate measurements

of particle spectra in the Earth's orbit using the PAMELA space experiments (Adriani et al. 2013) and AMS-02 (Aguilar et al. 2018).

The measurements onboard the PAMELA and AMS-02 spacecraft are carried out in a wide range of rigidities for quite a long time and make it possible to calibrate all ground-based detectors. Joint consideration of the spacecraft measurements with the results of ground-based monitoring of cosmic rays makes it possible to calibrate ground-based detectors and cover six cycles of solar activity since the beginning of ground-based CR monitoring in the 1950s.

While studying modulation for historical period from the Middle Ages to the present (McCracken 2007; McCracken et al. 2007) one can follow the time variations of the residual modulation for some effective energy. The cosmogenic data method makes it possible to obtain the residual modulation retrospectively temporal changes, but this method does not allow studying the residual modulation energy dependence. To study the residual modulation on the energy scale, it is necessary to use direct methods based on knowledge of the particles energy spectra outside the heliosphere (LIS spectra) and in the Earth's orbit. Experimental spectra outside the heliosphere were obtained using direct measurements of Voyager-1/2. Particle spectra have been measured on the Earth orbit by the AMS-02 spectrometer only since 2011. For earlier periods it is necessary to use ground-based data from various detectors that have been continuously monitoring since the middle of the last century. These are stratospheric measurements, monitoring of the neutron and muon components.

These data make it possible to consider the problem of cosmic rays residual modulation during the periods of a "quiet" Sun in order to evaluate and study quiet heliosphere modulation properties.

Studies of residual modulation on the time and energy scales are important for solving several inter-related problems: 1) determining modulation dynamics in the heliosphere of the "calm" Sun and its numerical evaluation; 2) the efficiency evaluation of the heliosphere as a whole and its individual regions; 3) verification of interstellar spectra various models of the nucleon component at low energies.

The aim of this work is to experimentally determine the spectra of the residual modulation for the last 6 solar cycles minima and to estimate the delay time of the cosmic ray response relative to the significant weakening period beginning of the heliospheric magnetic field.

2. The residual modulation determining method

The variation can be determined with respect to the selected base period of cosmic ray intensity $J_{Base} = J_{1AU}$ in the Earth's orbit (usually near the intensity maximum). In this case, the variation is defined as

$$v = J/J_{1AU} - 1, \quad (1)$$

where J is the calibrated (in this case, according to PAMELA data) intensity of cosmic rays outside the magnetosphere, obtained from the network data of a neutron monitors processed by the global spectrographic method (GSM) (Belov et.al. 2018), or from the data of individual detectors.

The variation can also be determined with respect to the unmodulated intensity of the local interstellar spectrum J_{LIS}

$$v_{LIS} = J/J_{LIS} - 1. \quad (2)$$

In (1) and in (2), the intensity is determined for one given particle rigidities. Variations v and v_{LIS} relative to different bases can be connected using the base conversion method.

Indeed, excluding J from (1) and (2), we obtain $J_{LIS}(v_{LIS} + 1) = J_{1AU}(v + 1)$. Then

$$v_{LIS} = \frac{J_{1AU}}{J_{LIS}}(v + 1) - 1 = v + \delta_{LIS}(v + 1), \quad (3)$$

where the variation relative to the LIS level is defined as

$$\delta_{LIS} = J_{1AU} / J_{LIS} - 1. \quad (4)$$

(For particles 10 GV (see table 1 below, model C2016) $\delta_{LIS} = 26.9/33.2-1=-19.0\%$).

Residual modulation is part of the total modulation, and the modulation depth is usually expressed as a positive number, so the residual modulation is $\Delta = |\delta_{LIS}|$.

The base values for each used detector were determined as annual average intensity values for the corresponding effective rigidity.

Or in another form

$$v_{LIS} = \frac{J_{1AU}}{J_{LIS}}(v + 1) - 1 = \frac{v - \delta_{1AU}}{1 + \delta_{1AU}} \approx v - \delta_{1AU}(v + 1), \quad (5)$$

where the variation already relative to the 1AU level is defined as

$$\delta_{1AU} = J_{LIS} / J_{1AU} - 1 \quad (6)$$

(for 10 GV particles $\delta_{1AU} = 33.2/26.9-1=23.4\%$).

Values of variation relative to the LIS level δ_{LIS} and relative to the 1AU level δ_{1AU} are connected as

$$\delta_{1AU} = -\frac{\delta_{LIS}}{\delta_{LIS} + 1} \approx -\delta_{LIS} \text{ for } |\delta_{LIS}| \ll 1.$$

3. Experimental data used

The results of the following detectors monitoring were used in the work:

PAMELA spectrometer data. For calibrating ground-based detectors and determining the basic intensity values the PAMELA magnetic spectrometer data turned out to be indispensable (Adriani et al. 2013; SSDC 2022; CRDB 2022; CRDB ultra 2022). It's operation period was on the 23/24 solar cycles minimum (2009).

The long-term detector stability and the average annual basic intensity values accuracy turned out to be sufficient for calibrating ground-based detectors (Belov et al. 2021). In addition, the PAMELA magnetic spectrometer measurements cover the detectors entire energy range we use. It is possible to use the results of magnetic spectrometers in sounding the stratosphere, but such measurements are carried out only for about 10 days during an annual expedition (Seo 2012; Maurin et al. 2020; CRDB balloon borne 2022). The average annual intensity values calibrated according to PAMELA data for 2009 and various effective rigidities R_{eff} are given in Table 1.

Ground detectors data at a distance of 1AU. These are the world network of neutron monitors (NM) data (NM Network 2022), muon telescopes (MT) data (Muon Network (GMDN) 2022), and stratospheric sounding of the ionizing component SS data (Balloon experiment 2022). The GSM global spectrographic method was carried out using data from the global NM network (Belov et.al. 2018). The result of this GSM analysis is the cosmic ray variations spectrum $v(R)$ outside the Earth's magnetosphere relative to the base period (in our case, 2009). To go to the cosmic rays intensity outside the magnetosphere, the NM network detector was calibrated using the PAMELA data for the period of 2009, i.e., calculated intensity $J = J_{\text{PAMELA}}(v_{1\text{AU}} + 1)$, where all values used depend on the particles rigidity (Belov et al. 2021). Other detectors (muon telescopes and stratospheric sounding) were calibrated in a similar way. The effective rigidities for the analyzed components are: charged component - $R_{\text{eff}}=4$ GV (Apatity and Mirny) and $R_{\text{eff}}=5.8$ GV (Moscow), muon component - $R_{\text{eff}}=41$ GV (vertical component for station Nagoya); detected particles effective rigidity for the neutron monitors ground-based network $R_{\text{eff}}=10$ GV.

LIS Spectra Models Data. The particles local interstellar spectrum is determining for calculating the cosmic rays intensity basic values outside the heliosphere for various detectors. The development of modern LIS models made it possible to estimate the residual modulation in a wide range of rigidities and to estimate their errors. There are dozens of interstellar cosmic ray spectra models made of different assumptions. We used only LIS models that relied on experimental data from Voyager-1 (Voyager Data 2022) for the lower range (<1 GV) and AMS-02 for the upper range (>100 GV) (CRDB ultra 2022). The particles modulation in the upper rigidity range was neglected, and therefore it was possible to use magnetic spectrometers on the Earth's orbit. We considered the following LIS spectra (in our notes): C2016 (Corti et al. 2016), B2019 (Bisschoff et al. 2019), B2020 (Boschini et al. 2020), V2015 (Vos & Potgieter 2015), and G1975 (Garcia-Munoz et al. 1975). The last LIS spectrum was obtained at the space age beginning. It is simple and well correlated with modern LIS measurements. Local stellar spectrum as a function of kinetic energy per nucleon $J_{\text{LIS}}^p(K)$ in units $(\text{m}^2 \text{ s sr GeV/nucleon})^{-1}$ for protons and helium nuclei is presented as

$$J_{\text{LIS}} = a(K_L + K)^{2.65}, \quad (7)$$

where $KL=b \exp(-K/K0)$ and the coefficients for the proton spectrum are defined as: $a=8900$, $b=0.78$, $K0=4$.

In Figure 1 (top panels) two models comparison of LIS rigidities spectra C2016 (Corti et al. 2016) and B2019 (Bisschoff et al. 2019) for protons and helium nuclei are made. The experimental data of Voyager 1 and the data of AMS-02high (CRDB ultra 2022) are also shown in the region of high rigidities, for which modulation can be neglected. For illustration, the modulated AMS-02 values are also shown (thin curve).

For comparison, we used only a pure power-law spectrum normalized at a rigidity of 976 GV according to the spectrometer data AMS-02 $J=8.571 \cdot 10^{-5}(R/976)^{2.82}$ in $(\text{m}^2 \text{ s sr GV})^{-1}$.

In Fig. 1, the arrows indicate the spectrum characteristic parts of the considered detectors - SS, GSM, MT. It is important that the rigidities range of 1-100 GV that is interesting for us (shaded area in Fig. 1) is in the spectrum region obtained only by interpolation, and therefore some uncertainty can be expected here. The bottom panel shows the ratios for the spectra $J_{\text{C2016}}/J_{\text{B2019}}$ and their dependence on rigidity; the discrepancy in the interest to us area reaches 10%.

Base intensities values $J_{1\text{AU}}$ and J_{LIS} for different rigidities R_{eff} by several LIS spectra data are given in Table 1.

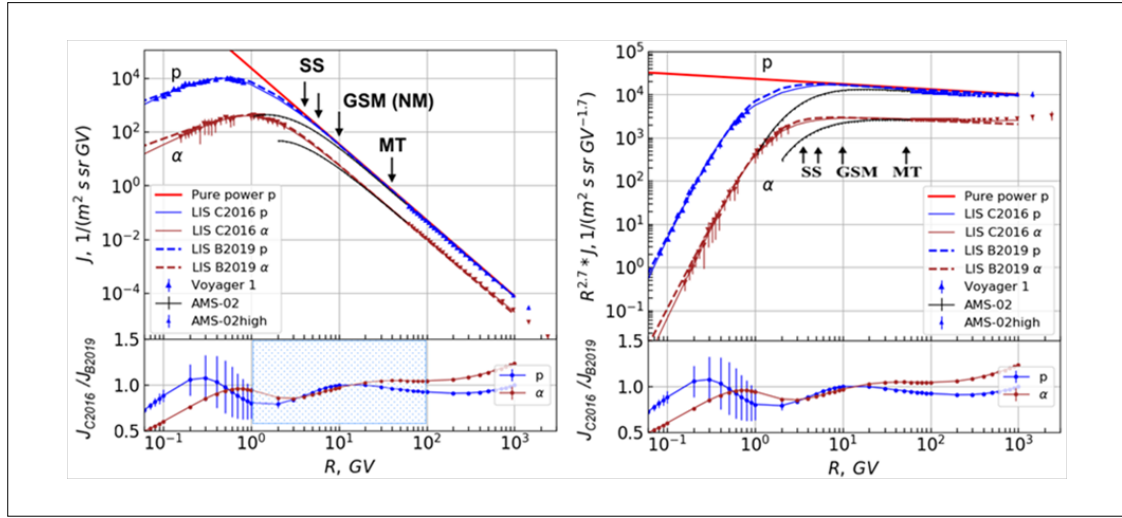


Fig. 1: Comparison of two LIS spectra models C2016 [Corti et al. 2016] and B2016 [Bisschoff et al. 2019] (upper panels) and their ratios (lower panels). The Voyager 1 [Voyager Data 2022] and AMS-02high [CRDB ultra 2022] data are also shown, from which the above mentioned spectra were obtained. The purely power-law spectrum of the protons is also shown.

Tab. 1: Base (2009) intensity values J_{1AU} , calibrated according to PAMELA, intensities J_{LIS} for different effective rigidities R_{eff} found for LIS spectra and result for residual modulation Δ .

Model of spectrum $p/(m^2 s sr GV)$	R_{eff} GV						
	Stratospheric Sounding			NM		MT	
	2.6	4.0±0.1	5.8±0.2	5	10±0.3	20	41±2.5
J_{1AU} (norm PAM, 2009)	578.984	250.042	106.015	149.932	26.869	4.183	0.569
J_{LIS} (C2016)	968.016	360.295	143.745	209.172	33.184	4.653	0.596
$\Delta = J_{1AU}/J_{LIS} - 1 , \%$	40.2	30.6	26.2	28.3	19.0	10.1	4.5
J_{LIS} (B2019)	1184.428	408.766	152.580	227.744	33.225	4.669	0.597
$\Delta, \%$	51.1	38.8	30.5	34.2	19.1	10.4	4.7
J_{LIS} (B2020)	1042.240	363.382	140.727	206.688	32.617	4.611	0.585
$\Delta, \%$	44.4	31.2	24.7	27.5	17.8	9.3	2.7
J_{LIS} (V2015)	1161.200	382.719	140.068	209.978	33.460	4.627	0.595
$\Delta, \%$	50.1	34.7	24.3	28.6	19.7	9.5	4.4
$\langle \Delta \rangle \pm \text{stat} \pm \text{sys}, \%$	46 ±0.3±5	34 ±0.3±4	26 ±0.3±3	30 ±0.3±3	19 ±0.4±2	10 ±0.5±2	4.0 ±0.7±2

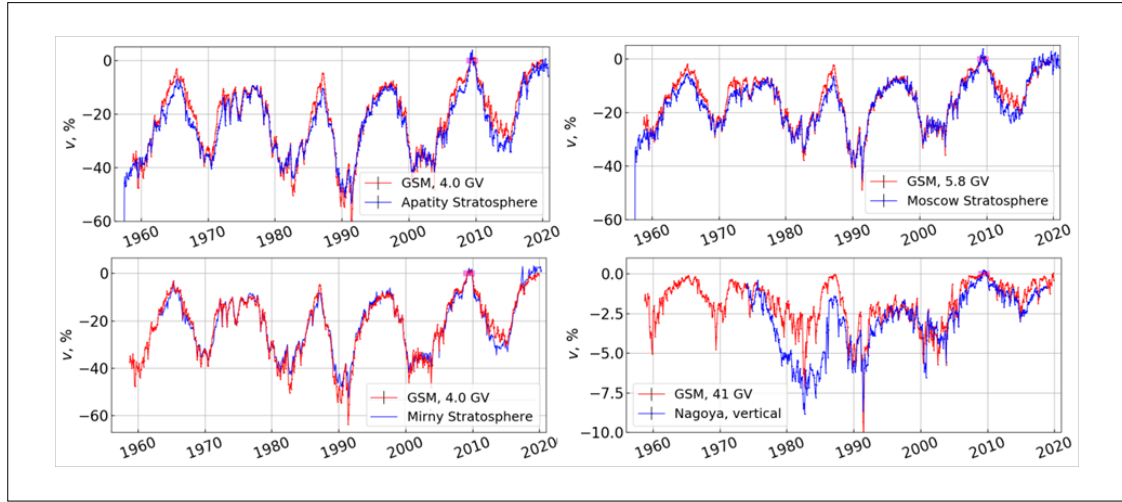


Fig. 2: Comparison of the observed variations in the charged and muon components with the results of a GSM analysis from a network of neutron monitors to determine the effective rigidity of each detector.

All the used ground-based detectors register cosmic rays with variable efficiency in a certain range of rigidities. For a comparative analysis it is necessary to have effective rigidities of each detector, the direct calculations of which are laborious and give ambiguous results, especially for the charged component. We made experimentally estimation of the effective rigidity R_{eff} , by comparing this detector variations and the neutron component $R_{eff}=10$ GV variations with the same effective rigidity R . It can be done knowing the cosmic ray variations spectrum determined by the GSM method from the data of a neutron detectors network, for example, in the work (Yanke et al. 2019). Found parameters a , γ , R_L of variation spectrum allow to determine variations for other rigidities as

$$v(R) = a_{10} \left(\frac{R_L + R}{R_L + 10} \right)^{-\gamma} \quad (8)$$

Such analysis results are shown in Fig. 2. The effective rigidities of the detectors under consideration are: for SS Apatity 4 ± 0.15 GV, for SS Mirny 4 ± 0.1 GV, for SS Moscow 5.8 ± 0.2 GV, and for MT Nagoya. V 41.0 ± 2.5 GV.

4. Discussion of results

To determine the residual modulation at any time, it is necessary to obtain the intensity J_{LS} by LIS spectra and intensity J_{IAU} at the base time for a given effective rigidities and calculate the residual modulation according to expression (4). The main results are shown in Table 1 were intensity and residual modulation values for various R_{eff} and for several LIS spectra models are given. Residual modulation for detectors with various effective rigidities is shown in Figure 3.

Each figure shows the temporal changes of cosmic ray variations relative to the 2009 base period. Variations were obtained from the calibrated intensities of each detector in accordance with (4). Variations relative to 2009 are indicated near the curves for all minima solar activity.

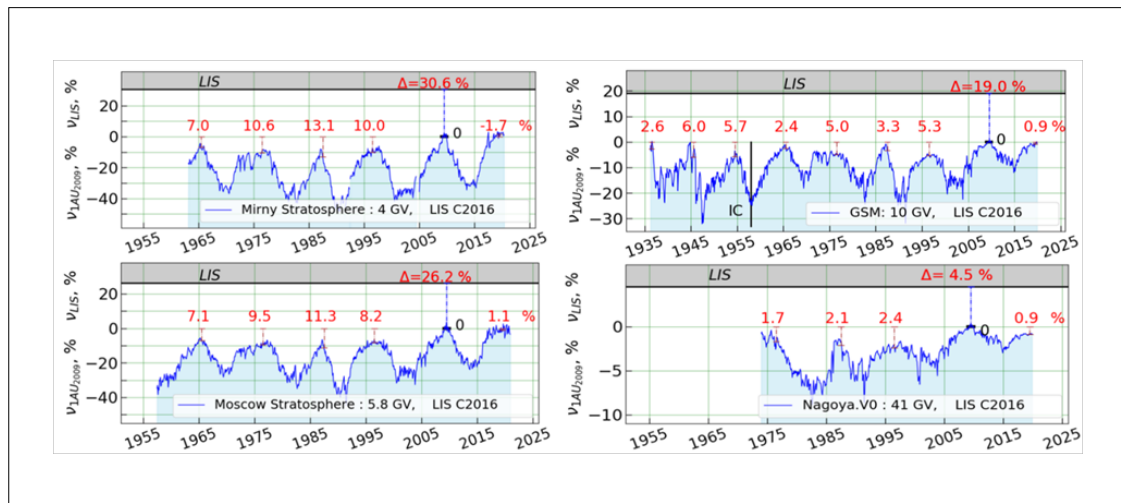


Fig. 3: A residual modulation Δ relative to the LIS level for detectors of various effective rigidities and variation relative to 2009 (curve numbers).

Fig. 3 also shows the residual modulation module Δ . Such estimates were made for several LIS spectra models (see Tab. 1), but the Fig. 3 shows the result only for the C2016 LIS spectrum (Corti et al. 2016).

The cosmic rays modulation analysis in the heliosphere showed that even during the period of the quietest Sun (for example, 2009), the residual modulation is significant. Thus, for 4.0 GV particles, the residual modulation averaged over all LIS spectra (the last line of Table 1) reaches $\Delta=34\pm 0.3(\text{stat})\pm 4(\text{sys})\%$ that is approximately equal to the modulation during the transition from minimum to maximum of solar activity. This is relevant for all rigidities. Similarly, for the rigidity of 41 GV (muon telescope) during the period of the quiet Sun, the cosmic rays residual modulation is $\Delta=4\pm 0.7(\text{stat})\pm 2(\text{sys})\%$, which is also comparable with the modulation from minimum to maximum of solar activity. Residual modulation values for other rigidities are given in Table 1.

Hence, the Sun in its most active phase is capable of modulating cosmic rays relative to quiet period, just as the quiet Sun is capable of modulating the local interstellar spectrum.

Knowing the residual modulation in the considered energy range, it is possible to form the residual modulation spectrum, i.e. the dependence of residual modulation on rigidity or energy. Such a spectrum is approximated by a power function, which is strongly modulated by an exponential function in the region of high rigidities:

$$\Delta = a_0 R^{-\gamma} \exp(-R/R_H), \quad (9)$$

It is shown in Figure 4 (left panel). The found values of the rigidity spectrum parameters for the residual modulation for the period of 2009 are equal to $a_0=(69.5\pm 1.1)\%$, $\gamma=(0.47\pm 0.05)$, $R_H=(37.7\pm 2.3)$ GV with multiple coefficient of determination $R^2=0.996$ and a small condition number of 30. At local points for rigidities of 5, 10, 20, and 41 GV (numbers in circles), the exponent of the power-law spectrum of residual modulation is ~ 0.3 , ~ 0.5 , ~ 0.9 , and ~ 1.3 , respectively. When approximating the modulation spectrum by the kinetic energy function K for the period of 2009, the parameters are determined as $a_0=(52.7\pm 1.1)\%$, $\gamma=(0.31\pm 0.08)$, $K_H=(29.3\pm 2.3)$ GeV with determination multiple coefficient $R^2=0.998$.

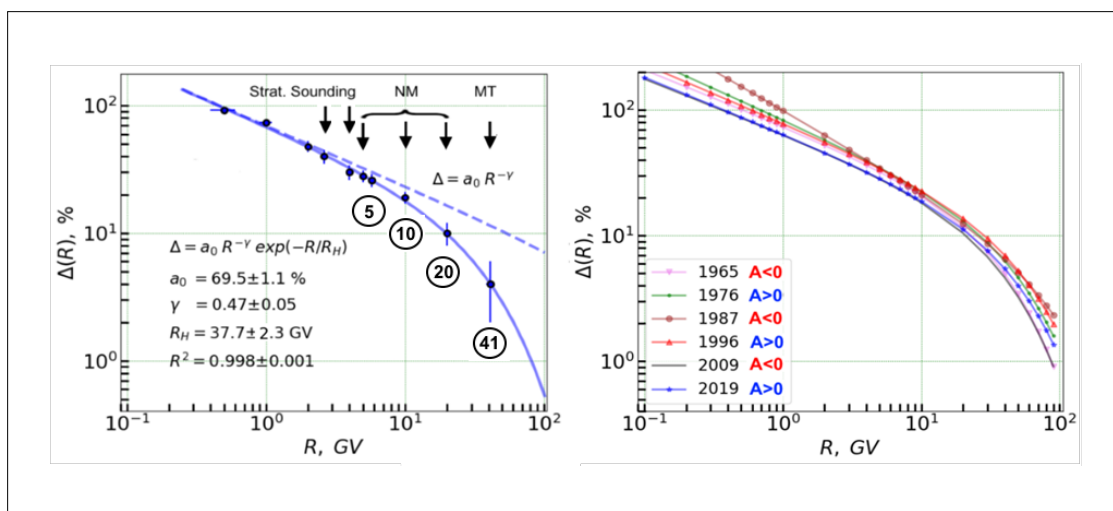


Fig. 4: Residual modulation spectrum and its approximation for the period of 2009 ($A < 0$) for the C2016 model [Corti et al. 2016] as a function of rigidity (left panel). Comparison of residual modulation spectra for various solar activity minima (right panel).

Let's consider the residual modulation spectrum behavior at different solar magnetic field polarities. The residual modulation spectra for 6 solar activity minima are shown in the right panel of Fig. 4. For any polarity, the rigidity spectrum is a power-law modulated by an exponential function in the region of high rigidities. This should be expected, since the residual modulation, in general, occurs in the far heliosphere, where the magnetic field is not even azimuthal, but is already highly turbulent. The dispersion of residual modulation values, for example, for 10 GV is about 5%, which agrees with the results shown on Figure 3.

A comparison can be made with the modulation spectrum on the Earth's orbit, determined in (Yanke et al. 2021). For the negative polarity of the solar magnetic field, such a spectrum is a power-law, modulated by an exponential function in the region of high rigidities, for positive polarity it is purely power-law. The reason is that in the first case, the particles enter the inner heliosphere through the neutral current sheet, in the second case - through the polar regions.

Above, we considered the residual modulation and its dependence on particle energy for the modern era, but its temporal changes in a historical perspective are also of interest.

5. Retrospectively determined residual modulation

Retrospectively, the residual modulation was discussed in (McCracken 2007; McCracken et al. 2007). This work was based on the combined instrumental neutron monitor data "pseudo-Climax" and cosmogenic isotope ^{10}Be data. The analysis shows that the intensity of cosmic rays steadily decreased; the residual modulation at solar cycle minima increased from 5% at the Spörer minimum in the 15th century to 18% at present for an effective rigidity of 10 GV.

Based on modern instrumental data, we obtained the residual modulation value $\Delta = 19 \pm 0.4(\text{stat}) \pm 2(\text{sys}) \%$, which resonates well with (McCracken et al. 2007).

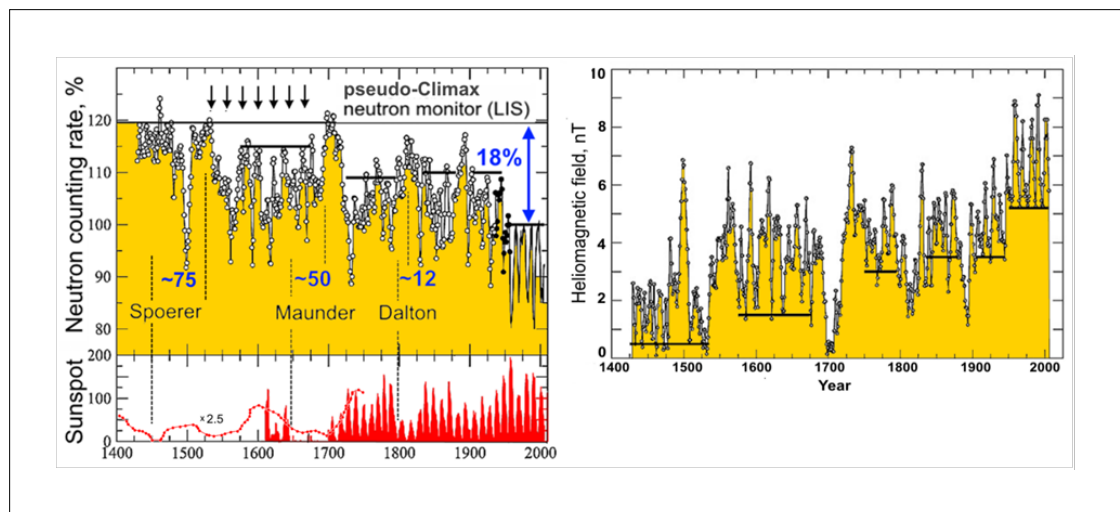


Fig. 5: Left panel - estimation (1428-1954) and observations (1951-2005) of neutron component variations for 10 GV. LIS line - calculated speed in the solar modulation absence [McCracken 2007; McCracken et al. 2007]. Solar activity indices for the period of the Middle Ages from 1400-1600 were obtained in [Usoskin et al. 2003]. Right panel - Heliomagnetic field near the Earth's orbit. The field was not obtained independently but reconstructed from the data of the previous figure of cosmic ray intensity in the heliosphere. [McCracken 2007a].

For a rigidity of 10 GV (neutron monitors), a residual modulation comparison and its time dependence is shown in Fig. 5 (left panel). A steady increase of the residual modulation is seen, which is a constant property of the galactic cosmic rays intensity on the Earth during the past five centuries.

The data in Figure 5 allow us to determine how long will it take the interstellar spectrum cosmic rays to fill the entire heliosphere if the Sun activity drops to zero.

Let's consider three known minima of solar activity: minimum of Spoerer, Maunder and Dalton.

The most famous, the Maunder minimum lasted from 1645 to 1715, and the cosmic rays intensity reached the LIS level around 1700, i.e. the delay time of the cosmic rays response to the Maunder minimum beginning is about 50 years. That is, the solar system is freed from the influence of the Maunder minimum for 50 years.

The Spoerer minimum lasted from 1415 to 1534, solar activity reached zero in ~1450, but cosmic rays reached a maximum on the Earth orbit only in ~1525 (the cosmic ray intensity reached a local maximum about 75 years later). On Fig. 5 (lower left panel) solar activity observed data are supplemented with reconstructed sunspot values for the Middle Ages by the method ^{10}Be analysis of Antarctic ice cores (Usoskin et al. 2003) (scaled by a factor of 2.5).

The Dalton minimum lasted from 1790 to 1830, but the cosmic rays intensity reached a local maximum after about 12 years, which is also noted in Fig. 5.

On Fig. 5 (right panel) shows the heliomagnetic field near the Earth's orbit (Caballero-Lopez et al. 2004). The results of this figure are based on cosmic ray intensity data (left panel) (McCracken 2007a). Three independent reconstructions of the heliomagnetic field (details in McCracken 2007) confirm this result. The most notable feature of Fig. 5 (right panel) is the steady long-term change in the interplanetary magnetic field between the 15th and 21st centuries from ~0.5 nT to the current level. Analyzing the results of Fig. 3 and Fig. 5, we can conclude that the cosmic rays residual modulation over the past 400 years has steadily increased to the current level.

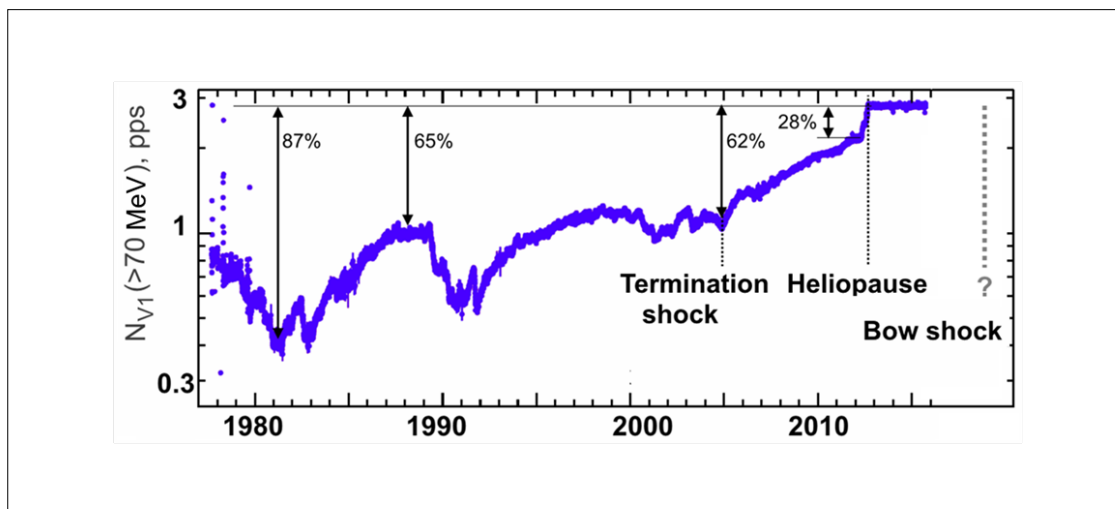


Fig. 6: Time dependence of the count rate of particles with energies >70 MeV according to Voyager-1 data [Cummings et al. 2016]. Estimation of modulation at key points of the Voyager-1 trajectory.

Based on the values of the residual modulation, we can consider two possibilities for realizing the radial dependence of the diffusion coefficient. With the active Sun, diffusion coefficient is $K \sim r$. Then, modulation $M \sim \ln(r)$ and, at velocity V_{sw} of the solar wind, according to the Parker model, the gradient is $dJ/dr = V_{sw}/K_0 \cdot J(r) \propto r^{-1}$, i.e. the modulation mainly occurs in the near heliosphere. With the quiet Sun, diffusion coefficient $K = const$. Then the modulation is linear $M \sim r$ and $grad(J) \approx 1\%/AU$. The modulation occurs throughout the entire heliosphere, and, hence, the calculated residual modulation is realistically achievable.

When analyzing the flattening of the spectrum at low energies (Fig. 1), the question may arise whether cosmic rays beyond the heliopause at a distance of 122 AU are subject to any modulation and what contribution does the region between the heliopause and the bow shock make? There are other uncertainties, some of which are discussed in (Kraimev et al. 2003; Krymsky et al. 1981).

Possible modulation of the cosmic rays outside the heliopause based on the magnetohydrodynamic model for the heliospheric medium was considered in (Strauss et al. 2013). It is shown that galactic CR modulation should persist beyond the heliosphere, where a positive CR gradient of $\sim 0.2\%/AU$ should be expected. Such a gradient can hardly be considered small, since it is not even an order of magnitude smaller than in the near heliosphere. As a result, modulation outside the heliopause can reach $25\% \div 40\%$ depending on the scenario determined by a set of CR modulation parameters. As a result, as suggested by the authors of (Strauss et al. 2013), the spectra measured by Voyager-1 are not yet true LIS spectra.

There may be another mechanism. The flattening of the CR spectrum may be due to the particles energy losses during their propagation in the Galaxy. For example, in (Werhahn et al. 2021), the stationary spectra of cosmic rays in a three-dimensional galaxy are calculated taking into account energy losses. The 3D MHD model self-consistently includes cosmic rays (protons, electrons, positrons). In the model, in particular, for protons, Coulomb and hadronic losses were taken into account and losses due to advection and diffusion (due to advection and diffusion) were estimated, provided that the diffusion coefficient depends on energy. The authors found that the spectra of protons above 10 GeV weakly depend on the

galactic radius, while at lower energies they acquire a radial dependence due to Coulomb interactions. The spectrum of protons below 1 GeV is flattened due to Coulomb interactions (which causes a spectral flattening) and turns into a reverse (a turn-over), which is consistent with the Voyager-1 data. The obtained stationary proton spectra provide excellent agreement with the observed spectra without the need for fine tuning over the entire range if the averaging was carried out for a height of 1 kpc.

Does residual modulation occur throughout the heliosphere? Direct measurements from Voyager 1 and 2 indicate that most of the residual modulation occurs between the shock wave that limits the supersonic flow of the solar wind and the heliopause. This can be seen in Fig. 6, which shows the count rate of a channel dominated by protons >70 MeV (with some fraction of electrons with energy >15 MeV) along the Voyager 1 route (Cummings et al. 2016). It can be seen that the modulation behind the shock front is comparable to the modulation from maximum to minimum in the 1980s. There are also theoretical considerations for this, since the perturbation of the medium increases behind the front of shock waves and stronger scattering and, hence, stronger modulation occurs.

6. Conclusions

1. An analysis of the modulation of cosmic rays into the heliospheres showed that even in the period of an exceptionally quiet Sun (2009), the residual modulation is significant for the entire range of rigidities under consideration (4 - 40 GV). For 10 GV particles, the residual modulation modulus is $\Delta = 19 \pm 0.4(\text{stat}) \pm 2(\text{sys}) \%$.
2. The spectrum of residual modulation at different polarities of the solar magnetic field can be described by a power function with an additional exponential dependence in the region of high rigidities.
3. The quiet Sun is capable of modulating the local interstellar spectrum by about the same magnitude as the Sun in its active phase of a relatively quiet period.
4. The resulting residual modulation for a rigidity of 10 GV is in good agreement with the results of the work based on combining data from a modern neutron monitor and cosmogenic isotope ^{10}Be data. The delay time of the response of cosmic rays relative to the moment of “disappearance” of the magnetic field of the Sun can be about 50 years.

Acknowledgments

The authors are grateful to the teams of the global network of cosmic ray stations that provide data (http://cr0.izmiran.ru/ThankYou/Our_Acknowledgment.pdf, last accessed June 27, 2023) on continuous registration of the neutron component; we thank the NMDB project (<http://www.nmdb.eu>). The work is carried out within the framework of the UNU “Russian Ground Network of Cosmic Ray Stations (CRS Network)”: <https://ckp-rf.ru/catalog/usu/433536> (last accessed June 27, 2023).

Questions and answers

Question 1: Flattening of the spectrum at low energies as a result of diffusion or energy losses - what is actually realized?

Answer 1: Both processes, but the flattening of the spectrum due to energy losses, apparently, dominates.

Question 2: Are there other options besides PAMELA data for calibrating ground detectors?

Answer 2: Yes, there is. For the period after 2011, AMS-02 data can be used; for the period from the 1970s, magnetic spectrometer data obtained during balloon measurements in the stratosphere can be used.

References

- Adriani, O. et al. (PAMELA Collaboration) 2013. Time Dependence of the Proton Flux Measured by PAMELA during the 2006 July-2009 December Solar Minimum, *ApJ*, 765, 91, <https://doi.org/10.1088/0004-637X/765/2/91>
- Aguilar, M. et al. (AMS Collaboration) 2018, Observation of Fine Time Structures in the Cosmic Proton and Helium Fluxes with the Alpha Magnetic Spectrometer on the International Space Station *Phys. Rev. Lett.*, 121, 051101, <https://doi.org/10.1103/PhysRevLett.121.051101>
- AMS-02 Data 2022, Space Science Data Center, <https://www.ssdsc.asi.it/ams>, <https://ams02.space/publications> (last accessed June 28, 2023)
- Belov, A., Eroshenko, E., Yanke, V., Oleneva, V., Abunina, M., Papaioannou, A., Mavromichalaki, E. 2018, The Global Survey Method applied to Ground Level Cosmic Ray Measurements *Solar Physics*, 293: 68, <https://doi.org/10.1007/s11207-018-1277-6>
- Belov, A.V., Gushchina, R.T., Shlyk, N.S., Yanke V.G. 2021, Using Data from a Ground-Based Network of Detectors and the PAMELA and AMS-02 Experiments to Compare Long-Term Variations in the Cosmic Ray Flux. *Bull. Russ. Acad. Sci. Phys.*, 85, 1039-1041, <https://doi.org/10.3103/S1062873821090045>
- Bischoff, D., Potgieter, M.S. and Aslam, O.P.M. 2019, New very local interstellar spectra for electrons, positrons, protons and light cosmic ray nuclei, <https://doi.org/10.3847/1538-4357/ab1e4a>
- Boschini, M.J., Della Torre, S., Gervasi, M., Grandi, D., Ohannesson, G.J., La Vacca, G., Masi, N., Moskalenko, I.V., Pensotti, S., Porter, T.A., Quadroni, L., Rancoita, P.G., Rozza, D., Tacconi, M. 2020, Inference of the Local Interstellar Spectra of Cosmic Ray Nuclei $Z \leq 28$ with the GALPROP-HELMOD Framework, <https://arxiv.org/abs/2006.01337v1>
- Caballero- Lopez, R.A., Moraal, H., McCracken, K.G., McDonald, F.B. 2004, The heliospheric magnetic field from 850 to 2000AD inferred from ^{10}Be records, *JGR*, 109, A12102, <https://doi.org/10.1029/2004JA010633>
- Corti, C., Bindi, V., Consolandi, C., and Whitman, K. 2016, Solar modulation of the local interstellar spectrum with Voyager 1, AMS-02, PAMELA and BESS, *Astrophys. J.*, 829:8, 9, <https://doi.org/10.3847/0004-637X/829/1/8>
- Cummings, A.C., Stone, E.C., Heikkila, B.C. et al. 2016, Galactic cosmic rays in the local interstellar medium: Voyager 1 observations and model results, *The Astrophysical J.*, 831:18 (21pp), No 1, <https://doi.org/10.3847/0004-637X/831/1/18>
- CRDB (Regular stratospheric sounding) 2022, https://sites.lebedev.ru/ru/DNS_FIAN (last accessed Dec 20, 2022)
- CRDB 2022, Cosmic Rays DataBase, Dec 20, 2022, <https://tools.ssdsc.asi.it/CosmicRays/chargedCosmicRays.jsp> (last accessed June 27, 2023)
- CRDB ultra 2022, Cosmic Rays DataBase, <https://lpsc.in2p3.fr/crdb/> (last accessed Dec 20, 2022). Description: Maurin D., Dembinski H., Gonzalez J., Maris Ioana C., Melot F. Cosmic-ray database update: ultra-high energy, ultra-heavy, and antinuclei cosmic-ray data (CRDB v4.0) *Universe* 2020, XX, 5; <https://arxiv.org/pdf/2005.14663.pdf> (last accessed June 27, 2023)
- Garcia-Munoz, M., Mason, G.M., Simpson, J.A. 1977, New aspects of the cosmic ray modulation in 1974-1975 near solar minimum, *Astrophys. J.*, V. 213, P. 263-268.
- Kraiev, M.B., Kalinin, M.S. 2003, Arguments in favor of the influence of the external electric field of the heliosphere on galactic cosmic rays, *Izv. RAS, ser. Phys.*, V.67, No. 10, P. 1439-1442.
- Krymsky, G.F., Krivoshapkin, P.A., Mamrukova, V.N., Skripin, G.V. 1981, Effects of interaction of the heliomagnetosphere with the galactic field in cosmic rays // *Geomagnetism and Aeronomy*. T. 21, No. 5. P. 923-925.
- Maurin, D., Dembinski, H., Gonzalez, J., Maris Ioana, C., Melot, F. 2020, Cosmic-ray database update: ultra-

- high energy, ultra-heavy, and antinuclei cosmic-ray data (CRDB v4.0) Universe 2020, xx, 5, <https://doi.org/10.48550/arXiv.2005.14663>
- McCracken, K.G., McDonald, F.B., Beer, J., Raisbeck, G., Yiou, F. 2004, A phenomenological study of the long-term cosmic ray modulation, 850–1958 AD, JGR, 109, A12103, <https://doi.org/10.1029/2004JA010685>
- McCracken, K.G. 2007, Long Term Changes in the Residual Modulation of the Galactic Cosmic Radiation, 30th ICRC, Mexico
- McCracken, K.G., Beer, J., 2007, Long-term changes in the cosmic ray intensity at Earth, 1428–2005. Journal of Geophysical Research Atmospheres, V.112, A10101, <https://doi.org/10.1029/2006JA012117>
- McCracken, K.G. (2007a), Helimagnetic field near Earth, 1428 – 2005, JGR, 112, A09106, <https://doi.org/10.1029/2006JA012119>
- Muon Network (GMDN) 2022, <http://cosray.shinshu-u.ac.jp/crest/DB/Public/Archives/GMDN.php> (last accessed June 27, 2023)
- Nagashima, K., Morishita I., 1980, Long term modulation of cosmic rays and invariable electromagnetic state in solar modulating region, Planet. Space Sci., V. 28 (2), P. 177–194, [https://doi.org/10.1016/0032-0633\(80\)90094-X](https://doi.org/10.1016/0032-0633(80)90094-X)
- Network NM 2022 <https://www.nmdb.eu>, <https://www.nmdb.eu/nest>, or <http://cr0.izmiran.ru/common> (last accessed Dec 20, 2022)
- Seo, E.S. 2012, Direct measurements of cosmic rays using balloon borne experiments, Astroparticle Physics, 39–40, 76–87. <https://doi.org/10.1016/j.astropartphys.2012.04.002>
- SSDC 2022, Space Science Data Center <https://www.ssdsc.asi.it> (last accessed Dec 20, 2022)
- Stone, E.C., Cummings, A.C., Heikkilä, B.C. et al. 2019, Cosmic ray measurements from Voyager 2 as it crossed into interstellar space. Nat Astron 3, 1013–1018, <https://doi.org/10.1038/s41550-019-0928-3>
- Strauss, R. D., Potgieter, M. S., Ferreira, S. E. S., Fichtner, H., Scherer, K. 2013, Cosmic ray modulation beyond the heliopause: a hybrid modeling approach, ApJ, 765, L18, <https://doi.org/10.1088/2041-8205/765/1/L18>
- Usoskin, I.G., Solanki Sami K., Schüssler Manfred, Mursula Kalevi, and Alanko Katja 2003, Millennium-Scale Sunspot Number Reconstruction: Evidence for an Unusually Active Sun since the 1940s, Phys.Rev.Lett, 91, 211101 <https://doi.org/10.1103/PhysRevLett.91.211101>
- Voyager Data 2022, Science Data Access, <https://voyager.jpl.nasa.gov/mission/science/data-access>, <https://voyager.jpl.nasa.gov>, <https://voyager.jpl.nasa.gov/mission/science/bibliography/crs> (last accessed Dec 20, 2022)
- Vos, E.E., Potgieter, M.S. 2015, New Modeling of Galactic Proton Modulation during the Minimum of Solar Cycle 23/24, Astrophys. J., 815, 119, <https://doi.org/10.1088/0004-637X/815/2/119>.
- Werhahn, M., Pfrommer, C., Girichidis, P., Puchwein, E., Pakmor, R. 2021, Cosmic rays and non-thermal emission in simulated galaxies. I. Electron and proton spectra compared to Voyager-1 data, Monthly Notices of the Royal Astronomical Society, V. 505, Issue 3, P.3273–3294, <https://doi.org/10.1093/mnras/stab1324>
- Yanke, V.G., Belov, A.V., Gushchina, R.T., Zirakashvily, V.N. 2019, The rigidity spectrum of the long-term cosmic ray variations during solar activity cycles 19–24. 26th Extended ECRS + 35th RCRC. SH33. Journal of Physics: Conference Series. 1181:012007, <https://doi.org/10.1088/1742-6596/1181/1/012007>
- Yanke, V.G., Belov, A.V., Shlyk, N.S., Kobelev, P.G., and Trefilova, L.A. 2021, The Experimental Spectrum of Variations of Cosmic Rays in a Wide Range of Hardness According to AMS-02 Data. Cosmic Research, V. 59, No. 6, P. 426–431, <https://doi.org/10.1134/S0010952521060101>

Open Access

This paper is published under the Creative Commons Attribution 4.0 International license (<https://creativecommons.org/licenses/by/4.0/>). Please note that individual, appropriately marked parts of the paper may be excluded from the license mentioned or may be subject to other copyright conditions. If such third party material is not under the Creative Commons license, any copying, editing or public reproduction is only permitted with the prior consent of the respective copyright owner or on the basis of relevant legal authorization regulations.